The Influence of Support Materials on The Photo-Fenton-like Degradation of Azo Dye Using Continuous Nanoparticles Fixed-bed Column

Zainab A. Mahmoud*   Mohammed A. Atiya**   Ahmed K. Hassan***

*, ***Department of Biochemical Engineering/ Al-Khwarizmi College of Engineering/
University of Baghdad/ Iraq
***Environment and Water Directorate/ Ministry of Science and Technology/ Baghdad/ Iraq
*Email: zainab.amahmoud@gmail.com
**Email: atiya@kecbu.uobaghdad.edu.iq
***Email: ahmedkhh71@gmail.com

Abstract

This study used a continuous photo-Fenton-like method to remediate textile effluent containing azo dyes especially direct blue 15 dye (DB15). A Eucalyptus leaf extract was used to create iron/copper nanoparticles supported on bentonite for use as catalysts (E@B-Fe/Cu-NPs). Two fixed-bed configurations were studied and compared. The first one involved mixing granular bentonite with E@B-Fe/Cu-NPs (GB- E@B-Fe/Cu-NPs), and the other examined the mixing of E@B-Fe/Cu-NPs with glass beads (glass beads-E@B-Fe/Cu-NPs) and filled to the fixed-bed column. Scanning electron microscopy (SEM), zeta potential, and atomic forces spectroscopy (AFM) techniques were used to characterize the obtained particles (NPs). The effect of two main parameters including contaminant flow rate concentration in continuous fixed-bed systems was investigated. To optimize both studied systems, the response surface methodology using the central composite design (CCD) was used. The analysis shows that the removal efficiency for GB-E@B-Fe/Cu-NPs was 81% and for glass beads-E@B-Fe/NPs was 62.6%.

Keywords: Glass beads; Fixed-bed column; Iron/copper nanoparticles; Granular bentonite; Photo-Fenton-like.

1. Introduction

Due to the extensive use of organic dyes in different industries, dyes are one of the most often discovered organic contaminants in natural waters. They are regularly identified in surface water, groundwater, and wastewater effluents [1]. Among the various dyes used in industries, azo dyes are the major proportion of these dyes and are difficult to degrade [2]. These organic dyes could react with other chemical compounds and produces hazardous and nonbiodegradable by-products. In addition, the presence of these dyes in water causes serious diseases such as cancer, splenetic sarcomas, and hepatocarcinoma [3].

As a result, there is increased interest in building a stable procedure for removing these azo dyes from water. There has been extensive investigation on the ability of physical methods (adsorption, reverse osmosis, membrane filtration, and ion exchange) and biological degradation (aerobic and anaerobic microbial degradation and enzymic degradation) to remove these non-destructive organic dyes [4]. However, these methods have drawbacks such as, the difficult and slow procedure of biological degradation whereas

physical methods are typically non-destructive or ineffective [5].

Hydrogen peroxide is decomposed by ferrous ions (Fe^{+2}) in the Fenton process, releasing hydroxyl free radicals •OH, which are regarded as a powerful oxidizing agent [6]. This method is advantageous because it requires minimal resources and has a short treatment time [7]. But it also has some drawbacks, like a narrow pH, high secondary waste mainly Fe^{+3}, and difficulty restore the catalyst (Fe^{+2}) [8]. To solve the challenges, the heterogeneous Fenton is suggested as an effective environmentally friendly, and inexpensive process [10].

In general, zero-valent iron (ZVI-NPs) achieved great success in heterogeneous Fenton-like processes due to the ease and cheapness of preparing [11], and the production of Fe^{+2} enhanced by using ZVI-NPs [5]. Additionally, the activity of ZVI-NPs highly increase by depositing transition noble metals like copper, nickel, palladium, and silver on the surface of ZVI-NPs [12].

To enhance catalyst dispersity and avoid the aggregation it necessary to support the Nanoparticles of materials exhibit good thermal and mechanical stability. heterogeneous Fenton catalysts to have a high catalytic activity [17]. Bentonite possesses exceptional physicochemical properties, offers a high specific surface area, and is inexpensive [13] .

Water treatment may greatly benefit from coupling advanced oxidation and green catalysts. Green nanotechnology has received considerable attention in recent years [14]. Several chemical and physical methods are obtainable for production of metallic nanoparticles, but these methods have many problems and drawbacks such as use of hazardous chemicals as reducing agents, limited material exchanges, large energy requirements, ecological toxicity, and economic inefficiency [15]. As a result, there is an urgent need to find a method to create nanoparticles with high efficiency, low cost, and environmentally safe. Presently, an easy, sustainable, quick, and eco-friendly green synthesis method employing plant leaves extract use as alternative for other traditional methods [16]. The plant extract contains many

biomaterials like polyphenol, vitamin, flavonoids, polysaccharide, sugar, and alkaloids which represent secondary metabolites with redox ability [17]. In addition, these biomolecules are considered as a capping, and chelating agent covering the nanoparticles and prevents it nanoparticles from agglomeration [18].

Continues reactors are preferred for large scale wastewater operating units, it has also been established primarily in lab-scale studies and the fixed-bed reactor is an example of continuous system. This system is characterized by ease of catalyst separation from the liquid and regenerated, providing excellent industrial development opportunities [19]. The fixed-bed is easy to build and has a ideal flow pattern that allows for increased contact between the catalyst and the reactant and lower maintenance costs [20]. It is also easily scalable from the lab or pilot plant to full production levels. [21]. Once the process initiates, the oxidation reaction start and the contaminates are treaties as pass over the catalyst [12] .

The presents study involved the use of eucalyptus leaves extract for green synthesis of Iron/Copper nanoparticles loaded on bentonite (E@B-Fe/Cu-NPs). This catalyst was employed to investigate the degradation of direct blue dye (DB15) through continuous photo-Fenton-like process using fixed-bed column. The granular bentonite and glass beads as support materials for E@B-Fe/Cu-NPs in fixed-bed column.

2. Materials and Method
2.1. Chemicals and Reagents

The bentonite of 75μm particles size was brought from State Company for Mining Industry, Iraq. Leaves of the eucalyptus tree were gathered from Baghdad University, Iraq. The glass beads were brought from the glass workshop of the university of Baghdad. Other chemicals and their source are illustrated in Table 1. The direct blue 15 (DB15) dye was brought from Central Drug House Company (MW: 992.8 g/mol, λ max: 594 nm).
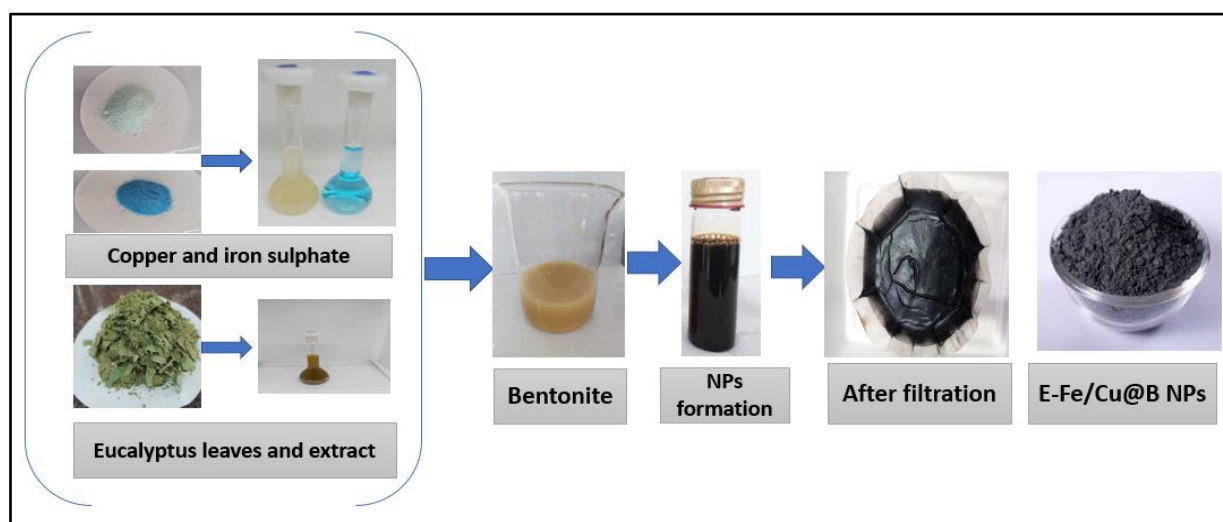
Table 1,
Chemicals and their sources.

Chemicals	Sources
Cupper sulfate (II) (CuSO$_4$.5H$_2$O)	Purchased from Alpha chemika company
Iron sulfate(II) (FeSO$_4$.7H$_2$O)	
H$_2$O$_2$ (30% w/v)	Purchased from the SDFCL company
Ethanol ($\geq$ 99.8%)	Purchased from Honeywell

2.2. E@B-Fe/Cu-NPs preparation

To remove dust and stuck dirt, eucalyptus leaves were gathered and washed. After a duration, the leaves were dried in a hot oven at 50 °C for 12 hours. The leaves were ground into a fine powder after they had completely dried and become crushable (size ranged between 1.4-2 mm). Following that, 10 g of eucalyptus leaf powder was added to 150 ml of deionized water and boiled for 30 minutes at 80 °C. After cooling. Thereafter, the vacuum filtration was used to filtrate the extract and eliminate any suspended leaves.

To finish the E@B-Fe/Cu-NPs preparation, 2 g bentonite was mixed into 100 ml deionized water and stirred for 30 minutes at room temperature. Meanwhile, salt solutions were made by dissolving 1.5 g of iron (II) sulfate and 0.4 g of copper (II) sulfate in 50 ml of deionized water. The salt solutions were then combined into the bentonite solution and stirred for 60 minutes in an ultrasonic vibration water bath. Then, with constant stirring, a 100 ml of eucalyptus extract was added gradually to the bentonite and salts mixture. After several drops of the extract were added, the color of the mixture changed from yellow to black, indicating that Fe^{+2} and Cu^{+2} were reduced to zero-valent [22]. Following that, the black precipitate of E@B-Fe/Cu-NPs was vacuum filtered and washed directly with distilled water, followed by absolute ethanol. The E@B-Fe/Cu-NPs were then dried at room temperature overnight before being ground into a fine powder with a mortar. Figure 1 depicts the steps for preparing E@B-Fe/Cu-NPs.

Fig. 1. E@B-Fe/Cu-NPs preparation steps.

2.3. Characterization of E@B-Fe/Cu-NPs

The resultant nanoparticles were characterized using scanning electron microscopy (SEM) to specify the size and shape. While the chemical compositions were analysed through energy dispersive x-ray spectroscopy (EDAX). The zeta potential was used to determine stability of E@B-Fe/Cu-NPs in collide suspension. The morphology and surface roughness of E@B-Fe/Cu-NPs were specified through atomic force spectroscopy (AFM).

2.4.Design of photoreactor

To design a photoreactor an aluminium cylindrical container with diameter of 40 cm and length 50 cm was used to install the lamps on it and to provide a reflective surface. Twenty-four lamps were used these lamps emit UV light type A with intensity of 1 W/m2 and wavelength of 365 nm. The distance between the lamps and the reaction cell was fixed at 10 cm. To prevent the outside light from entering the reactor, the cylindrical container was placed inside Opaque wooden box with dimensions of (60*60*60 cm). Two cooling fans were used to keep the temperature inside the reactor at required value. Moreover, the thermocouples used to observe the temperature during the reaction. The schematic diagram of the photoreactor is shown in Figure 2
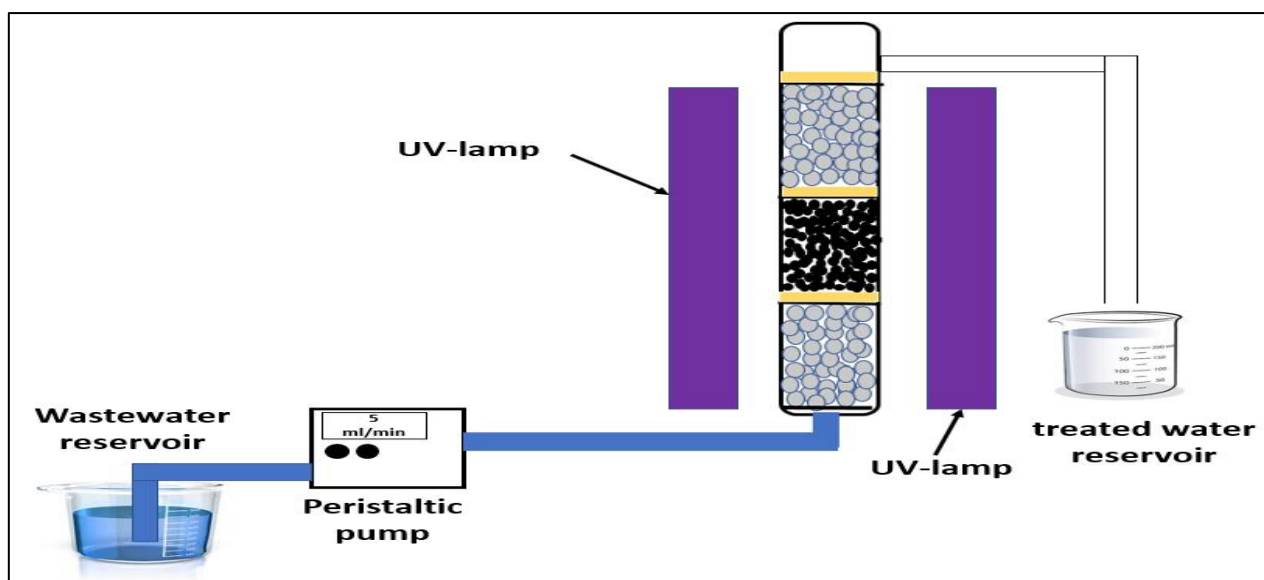

Fig. 2. Schematic diagram of continuous photo-Fenton-like process using fixed-bed column.

2.5. Fixed-bed Experiment

The fixed-bed experiments were performed using Pyrex column (33 cm length, 2.2 cm diameter). The removal of DB15 through fixed-bed column were examined using two different fixed-bed arrangements illustrated in Figure 3 a, b. To provide a uniform velocity profile for passing fluid, glass beads (size 1-1.5 mm) were packed. A 1 g of catalysts was held on granular bentonite (size 1-1.5 mm) and packed in the column, Figure 3a. The glass beads also used to fill the upper part of the column and occupy space of (10 cm thickness). The other column arrangements (Figure 3b) involved mixing 1 g of E@B-Fe/Cu-NPs with glass beads of size (0.5-1 mm). The stock solution of 1000 mg/L of dye was prepared and used to prepared required dye concentrations. The pH of solution was adjusted to 3.5 and H_2O_2 dosage of 7.5 mmol/L was added to the DB15 solution. To initiate the experiment, the column fixed at the centre of photoreactor while the inlet DB15 solution kept in dark box and a peristaltic pump was used to pumping the contaminant solution through the column.   Before started the experiments, the column is filled with glass beads only to check if there is any effect or removal of dye, the results indicate that the glass beads alone do not affect dye removal, Thereafter, the column is filled with glass beads, and 8 cm granular bentonite (without E@B-Fe/Cu-NPs) to check if the bentonite affect the removal of dye, A 57.5 g/L dye concentration (without H_2O_2) was pumped into the column and the outlet concentrations were checked. The removal efficiency does not exceed (17%) with a q_{total} of (0.629 mg) only. This result indicates that both the adsorption and the Fenton processes occurred when E@B-Fe/Cu-NPs mixed with granular bentonite.
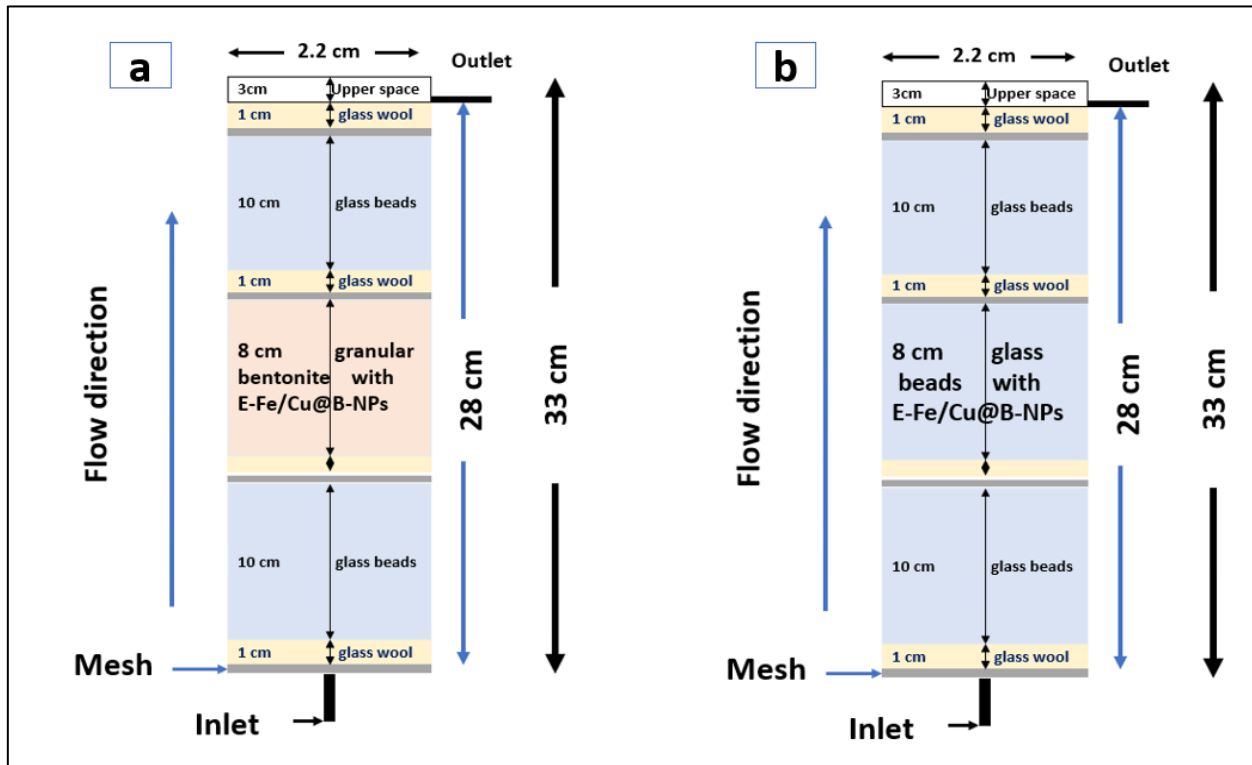
Fig. 3. (a) Fixed-bed column of GB-E@B-Fe/Cu-NPs, (b) fixed-bed column of glass beads- E@B-Fe/Cu-NPs

2.6. Design of Experiments

Response surface methodology (RSM) is a statistical method being useful for the optimization of processes and widely used for experimental design. RSM is useful tool help to understand the relationship between parameters and their effect on responses [23]. optimization the process by RSM is more efficient for analysing experimental results rather than the conventional one-factor-at-a-time approach. In this study, Central Composite Design (CCD) was employed for the optimization of continuous Photo-Fenton-like treatment of DB15 wastewater. A four-factorial, five-level CCD consisting of 10 experiments was performed in the present work, including two replications at the canter point [24]. Flow rate and Initial DB15 concentrations were considered as the independent variables while DB15 removal efficiency was considered as the responses. Table 1. Illustrate the parameters studied and their ranges. Additionally, the ANOVA parameters such as probability (P-value) and Fisher-test (F-value) were used to demonstrate how the parameters affect the responses [25]. the predicted R^2 must be in reasonable agreement with the adjusted R^2 to confirm that adjusted responses are in agreement with predicted one [26]. Eq.1 state the polynomial equation suggested by the design software and it illustrates the relationship between the independents dependents variables [4].

$$y = \alpha_o + \alpha_1 x_1 + \alpha_2 x_2 + \alpha_3 x_3 + \alpha_4 x_4$$
$$+ \alpha_{11} x_1^2 + \alpha_{22} x_2^2 + \alpha_{33} x_3^2$$
$$+ \alpha_{44} x_4^2 + \alpha_{12} x_1 x_2$$
$$+ \alpha_{13} x_1 x_3 + \alpha_{14} x_1 x_4$$
$$+ \alpha_{23} x_2 x_3$$
$$+ \alpha_{24} x_2 x_4 \qquad \dots (1)$$

Where y is the response, α_o is the constant of the regression equation, $\alpha_1, \alpha_2, \alpha_3, \alpha_4$ is linear coefficients, $\alpha_{12}, \alpha_{13}, \alpha_{23}, \alpha_{24}, \beta_{14}$ is the interaction coefficients, ($\alpha_{11}, \alpha_{22}, \alpha_{33}, \alpha_{44}$) is the quadratic coefficients and x1, x2, x3, x4 are the independent variables.

Table 2,
Ranges and levels of parameters studied through continues photo-Fenton-like process

Parameters	Ranges and levels				
	-α	Low (-1)	Middle (0)	+α	High (+1)
Flow rate (ml/min)	0.172	1	3	5.829	5
DB15 concentration mg/L	9.466	25	62.5	115.533	100

2.7. Fixed-bed results analysis

The removal efficiency in fixed-bed design is assess from breakthrough curve. The breakthrough curve involves drawing of time against ratio of initial DB15 concentration to outlet concentration (C_t/Co). The other important parameter that obtained from breakthrough curve is breakthrough time (t_b) is the time require for the effluent to reach 0.05 of the initial dye concentration [27]. Moreover, the treatment process stopped when the ratio of C_t/Co reached 0.9 and the time at this point called execution time (t_e) [29]. In addition, the total amount of dye removed by the fixed-bed column could be estimated graphically from the area above the breakthrough curve as given in Eq. 3 [27].

$$qtotal = \frac{QA}{1000} = \frac{QCo}{1000}\int_{t=0}^{ts}\frac{Ct}{Co}dt \qquad \ldots (2)$$

Where A is the area above the curve, Q is the flow rate of contaminant solution (ml/min), Co and Ct are the initial dye concentration and outlet dye concentration (mg/L) respectively, and t_s is saturation time.

$$mtotal = \frac{CoQts}{1000} \qquad \ldots (3)$$

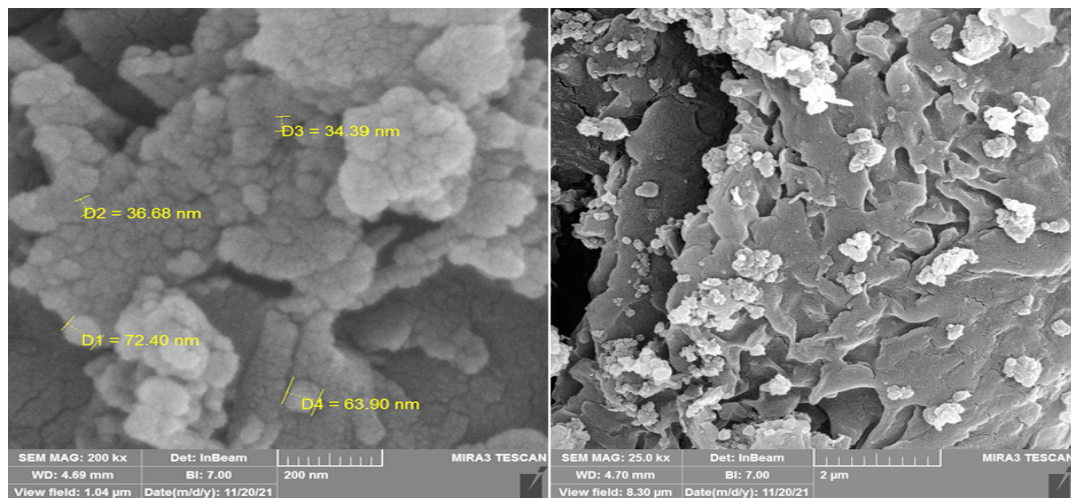$$RE\% = \frac{qtotal}{mtotal}*100 \qquad \ldots (4)$$

m_{total} represent the total amount of contaminant entering the column and RE% is the total removal efficiency [30]

3. Results and Dissection
3.1. Characterization of E@B-Fe/Cu-NPs

The SEM analysis of E@B-Fe/Cu-NPs shown in Figure 4 revealed that the NPs had a spherical shape and porous surface, with a diameter of approximately from (34.39-72.40nm). Furthermore, the uniform distribution of NPs on the surface of bentonite is demonstrated, which prevents NP agglomeration [31].

Furthermore, the EDAX analysis revealed the constituents and chemical constituents of E@B-Fe/Cu-NPs. EDAX analysis revealed peaks of Si, Fe, Cu, C, O, Na, Mg Al, Ca, and S, as shown in Figure 5. C and O, on the other hand, were referring to the existence of polyphenolic compounds and other organic matter in eucalyptus leaf extract [32]. Furthermore, the peaks Si, Mg, Al, Na, Ca , and S appeared as a result of the NPs being supported by the calcium bentonite clay [31].

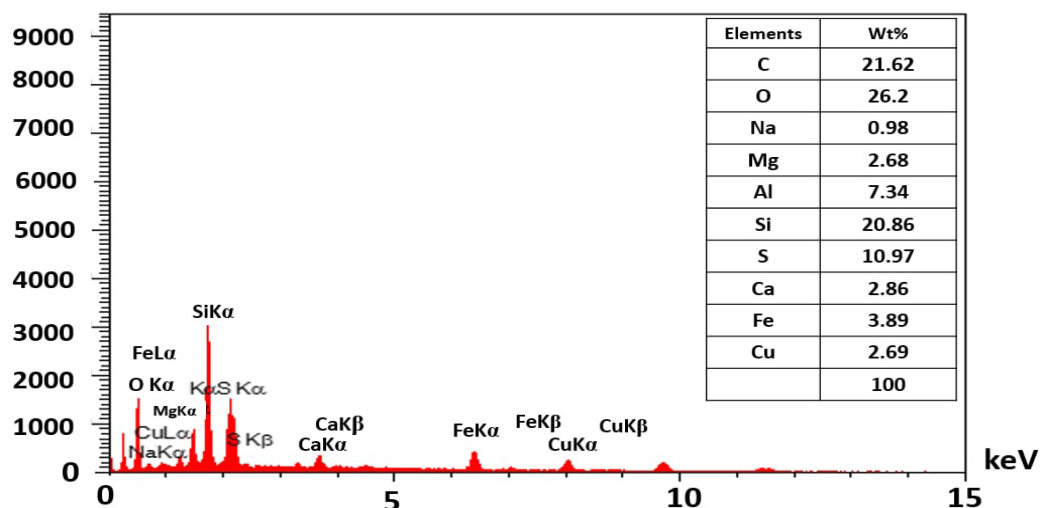**Fig. 4. The SEM of E@B-Fe/Cu-NPs.**

Elements	Wt%
C	21.62
O	26.2
Na	0.98
Mg	2.68
Al	7.34
Si	20.86
S	10.97
Ca	2.86
Fe	3.89
Cu	2.69
	100

Fig. 5. The EADX analysis of E@B-Fe/Cu-NPs.

The surface charge of NPs in collide suspension were characterized using ZP measurement. In the ZP analysis ,a sharp peak at -73.52 mV was obtained as clarified in Figure 6.
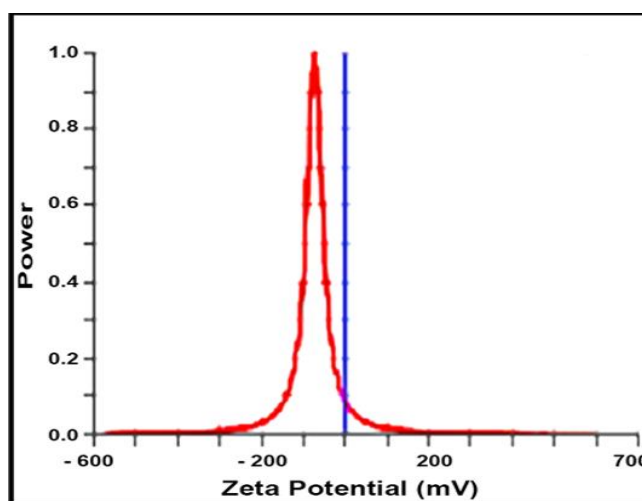

Fig. 6. Zeta potential of E@B-Fe/Cu-NPs.

It is observed that the surface of the NPs is negatively charged and dispersed in the medium. The high negative value confirms the repulsion among the particles, preventing the agglomeration of NPs and proving that NPs are very stable [33]. The stability of prepared catalyst is due to coating of NPs surface with polyphenol present in eucalyptus leaves [34].

The surface roughness is one of the important features required in catalysts to improve the catalytic process of H_2O_2. As shown in Figure 7 the high roughness can be seen on NPs surface [35]. Moreover, the NPs size ranged between (28-96 nm).
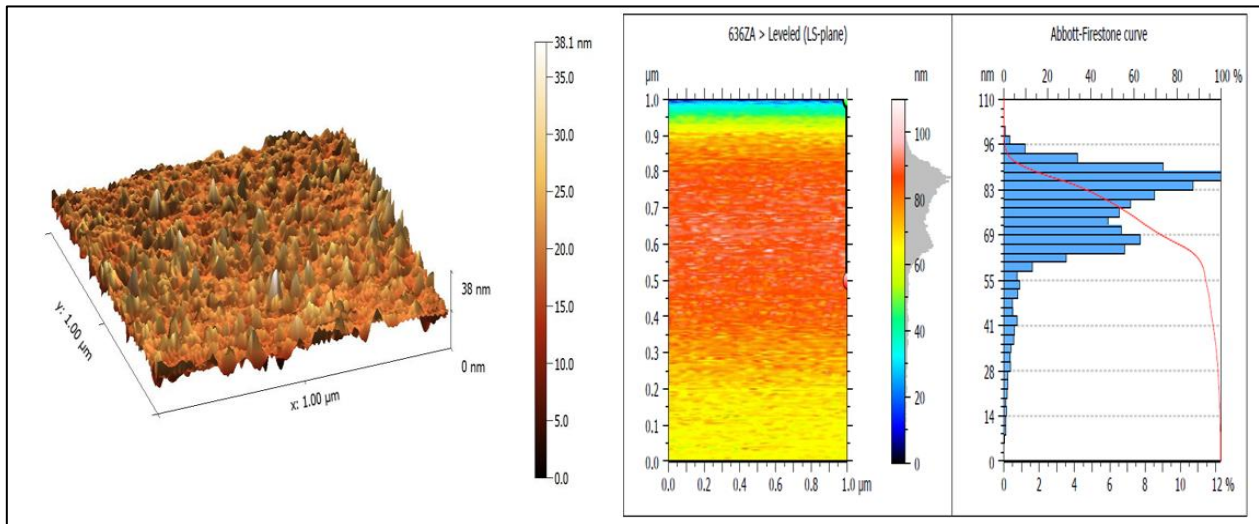
Fig. 7. Atomic force microscopy (AFM) characterization of E@B-Fe/Cu-NPs.

3.2.   Statistical analysis of continuous fixed-bed column containing GB-E@B-Fe/Cu-NPs

Table 3 lists the adjusted and predicted responses. These data were compared and analysed statistically by the CCD. The results in Table 4 indicates the predicted responses are compatible with adjusted responses because the difference between predicted R^2 and adjusted R^2 is less than 0.2 [1]. Figure 8 gives an evident for compatibility between these two responses.
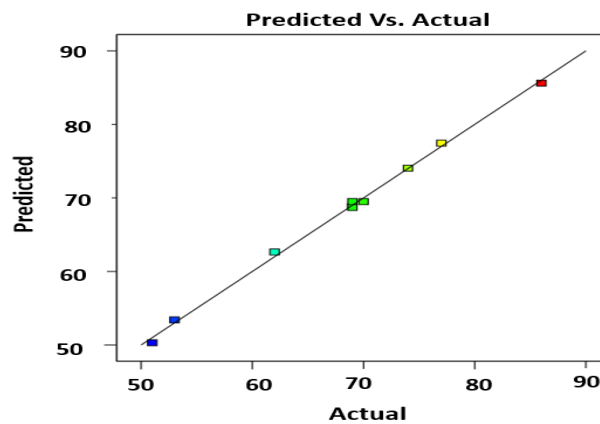

Fig. 8. Actual versus Predicted responses of GB-E@B-Fe/Cu-NPs experiments.

P-value is less than 5% indicates model terms are significant and as F-value increases the terms become more affected. As given in ANOVA analysis (Table 4), the P-value of flow rate was <0.0001and F-value of 1446.39 indicate that flow rate has a significant effect on response and it more affected than DB15 concentration [26]. Interaction effect between flow rate and DB15 concentration gas a significant effect on responses.

In addition, the regression coefficient of the quadratic model was (0.998) which indicates that the quadratic model well matches continuous photo-Fenton-like experiments [4]. The ANOVA analysis illustrated that the F-value and P-value of the model were 391.08 and < 0.0001, respectively, which indicates the model is significant. The quadratic model for DB15 removal obtained through continuous photo-Fenton-like experiments is given in Eq. 5.

$$\%DR = 69.5 - 9.6A + 1.88B - 6.5AB - 2.81A^2 + 0.9375B^2 \qquad \dots(5)$$

Table 3,
Actual and Predicted responses of continuous fixed-bed column containing GB-E@B-Fe/Cu-NPs.

Run	A:Flow rate (ml/min)	B:DB15 concentration (mg/l)	Actual responses (%)	Predicted response (%)
1	3	115.533	74	74.04
2	5.82843	62.5	51	50.30
3	3	9.46699	69	68.71
4	0.171573	62.5	77	77.45
5	3	62.5	69	69.50
6	1	100	86	85.61
7	3	62.5	70	69.50
8	5	100	53	53.41
9	1	25	69	68.84
10	5	25	62	62.64

Table 4,
ANOVA for quadratic model of fixed-bed column containing GB-E@B-Fe/Cu-NPs.

Source	Sum of Squares	df	Mean Square	F-value	p-value	Comments
Model	995.96	5	199.19	391.08	< 0.0001	significant
A-Flow rate	736.70	1	736.70	1446.39	< 0.0001	
B-DB15 concentration	28.39	1	28.39	55.74	0.0017	
AB	169.00	1	169.00	331.81	< 0.0001	
A^2	36.16	1	36.16	71.00	0.0011	
B^2	4.02	1	4.02	7.89	0.0484	
Residual	2.04	4	0.5093			
Lack of Fit	1.54	3	0.5124	1.02	0.6039	not significant
Pure Error	0.5000	1	0.5000			
Cor Total	998.00	9				
R^2	0.998					
Adjusted R^2	0.995					
Predicted R^2	0.987					
Adeq. precision	63.857					
Std.Dev.	0.7137					

3.3. Effect of parameters on continuous fixed-bed experiments using GB-E@B-Fe/Cu-NPs

3.3.1. Interaction effect between flow rate and DB15 concentration

According to Figure 9, increasing the flow rate from 1 to 5 ml/min led to decreasing the removal efficiency. Also, Table 5 shows that the breakthrough time t_b, saturation time t_s and execution time t_e increased with increasing the flow rate. This phenomena occur, due to increasing residence time of contaminant in the column with decreasing flow rate [36].

Furthermore, as DB15 concentration risen from 25 to 100 mg/L, tb, ts, and te decreased. This happens because dye molecules obstruct the catalytic process of H_2O_2 by blocking catalyst pores and thereby preventing the formation of •OH. Despite using the same amount of H_2O_2, when the DB15 concentration was 25 mg/L, the ratio of •OH to initial DB15 concentration was greater, indicating strong removal efficiency and a longer breakthrough time. This helps to explain why low initial DB15 concentrations have a longer breakthrough time and a high removal efficiency [37]. Figures 10 and 11 depict the breakthrough curves.
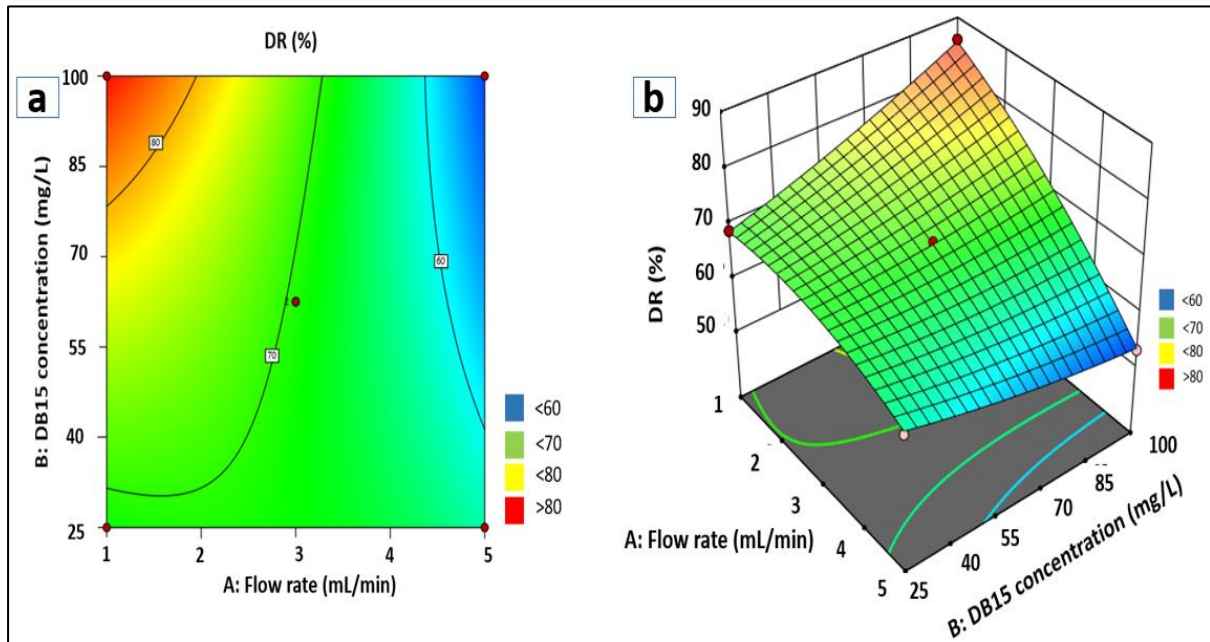
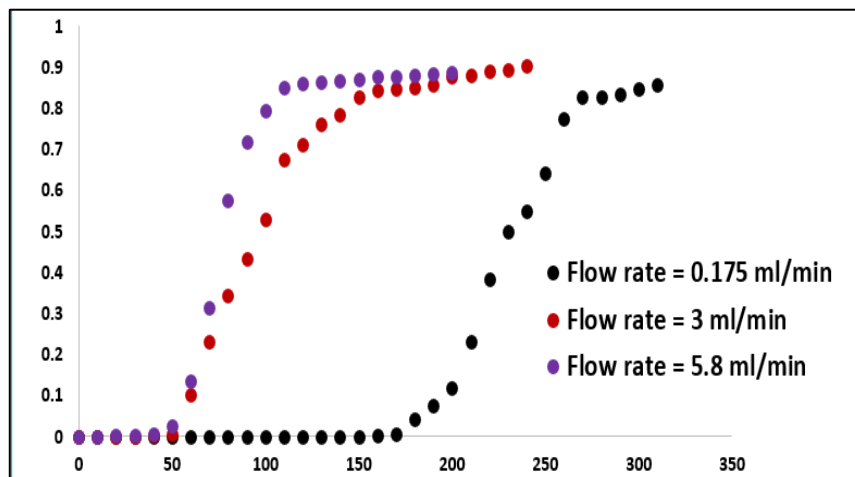**Fig. 9. (a) Contour plot (b) 3Dsurface of fixed-bed column containing GB-E@B-Fe/Cu-NPs.**

Fig. 10. The breakthrough carves at constants DB15 concentration of 626.5 mg/L for fixed-bed column containing GB-E@B-Fe/Cu-NPs.
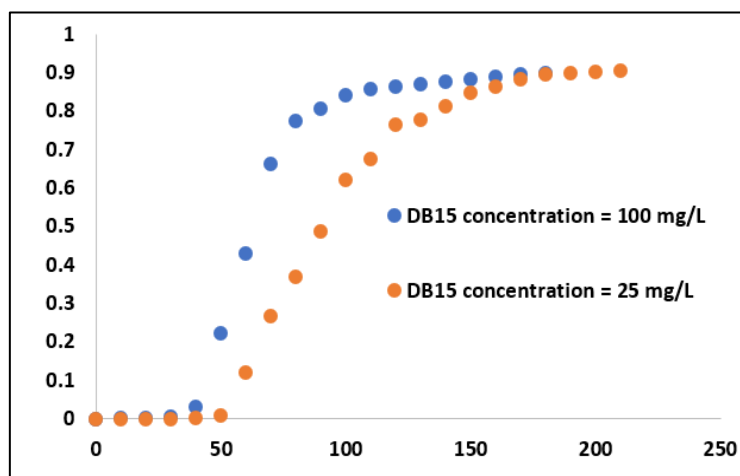

Fig. 11. The breakthrough carves at constants flow rate of 5 ml/min for fixed-bed column containing GB-E@B-Fe/Cu-NPs.

Table 5,
The results of breakthrough curve for fixed-bed column containing GB-E@B-Fe/Cu-NPs.

EXP. No.	A: Flow rate ml/min	B:DB15 concentration mg/L	DR %	m_{total} mg	q_{total} mg	t_b min	t_s min	t_e min
1	3	115.533	74	95.497	70.924	28.3	132.6	179.3
2	5.82843	62.5	51	49.88	25.503	38	97.4	190.5
3	3	9.46699	69	3.618	2.477	122.1	175.3	255.6
4	0.171573	62.5	77	2.873	2.22	162.3	287	371.1
5	3	62.5	69	31.841	21.873	42.6	161.5	235.1
6	1	100	86	22.109	19.612	96.4	277.3	312.6
7	3	62.5	70	31.57	22.252	44.1	164.3	233.1
8	5	100	53	60.54	32.038	26.1	90.6	171.2
9	1	25	69	6.428	4.45	155.7	254.8	368.1
10	5	25	62	11	17.68	48.9	126.3	202.5

3.4. Statistical analysis of continuous fixed-bed column containing glass beads-E@B-Fe/Cu-NPs

Table 6 lists the adjusted and predicted responses obtaining fixed-bed experiments. These data were compared and analysed statistically by the CCD. The ANOVA analysis (Table 7) indicates the predicted responses are compatible with adjusted responses with predicted R^2 and adjusted R^2 were 0.988 and 0.974, respectively. Figure 12 gives an evident for compatibility between these two responses.
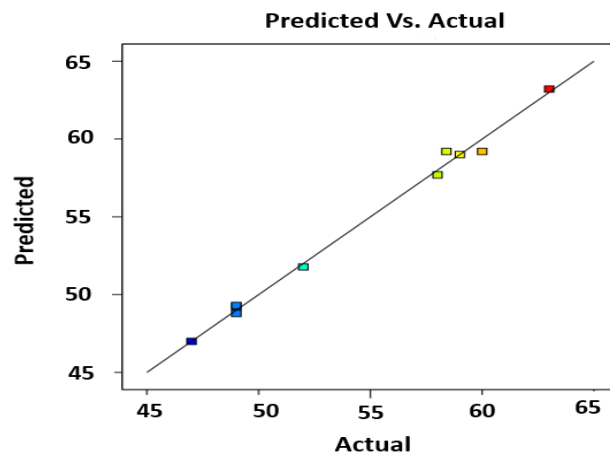

Fig. 12. Actual versus Predicted responses for fixed-bed glass beads-E-Fe/Cu@B-NP

Table 6,
Adjusted and predicted responses obtaining from fixed-bed glass beads-E@B-Fe/Cu-NPs

Run	A:flow rate (ml/min)	B:dye concentration (mg/L)	Adjusted response (%)	Predicted response (%)
1	5	100	49	48.79
2	3	62.5	60	59.20
3	3	62.5	58.4	59.20
4	1	25	63	63.21
5	3	115.533	47	46.99
6	5.82843	62.5	49	49.31
7	5	25	52	51.78
8	0.171573	62.5	58	57.69
9	3	9.46699	59	59.01
10	1	100	49	49.22

Table 7,
ANOVA for quadratic model of fixed-bed glass beads-E@B-Fe/Cu-NPs.

Source	Sum of Squares	df	Mean Square	F-value	p-value	
Model	301.77	5	60.35	146.02	0.0001	significant
A-flow rate	70.38	1	70.38	170.27	0.0002	
B-dye concentration	144.25	1	144.25	348.99	< 0.0001	
AB	30.25	1	30.25	73.19	0.0010	
A²	37.13	1	37.13	89.83	0.0007	
B²	43.93	1	43.93	106.29	0.0005	
Residual	1.65	4	0.4133			
Lack of Fit	0.3733	3	0.1244	0.0972	0.9509	not significant
Pure Error	1.28	1	1.28			
Cor Total	303.42	9				
R²	0.995					
Adjusted R²	0.988					
Predicted R²	0.974					
Adeq. precision	32.56					
Std. Dev.	0.643					

In this experiments, DB15 concentration exhibit higher effect on response than flow rate with P-value and F-value of <0.0001 and 348.99 while the P-value and F-value of flow rate were 0.0002 and 170.27. In addition, the quadratic model well matches continuous photo-Fenton-like experiments using glass beads with regression coefficient of 0.995. The ANOVA analysis illustrated that the F-value and P-value of the model were 146.02 and < 0.0001, respectively, which indicates the model is significant. The quadratic model for DB15 removal obtained through continuous fixed-bed experiments is given in Eq. 6

$$\%DR = 59.2 - 2.97\,A - 4.25B + 2.75AB - 2.85A^2 - 3.1B^2 \qquad ...\,(6)$$

2.1. Effect on parameters on continuous fixed-b-ed experiments containing glass beads-E@B-Fe/Cu-NPs

2.1.1. Interaction effect between flow rate and DB15 concentration

In fixed-bed experiments packed with glass beads and E@B-Fe/Cu-NPs, the DB15 concentration exhibited a greater influence as compared to the experiments carried out in column packed with bentonite and E@B-Fe/Cu-NPs, where flow rate showed a substantial impact on the removal efficiency. Furthermore, Table 8 and Table 5 shows 47 % and 74% removal efficiency at flow rate 3ml/min, DB15 concentration 115.553 mg/L for glass beads and bentonite experiment respectively. Otherwise, the removal efficiencies in both experiments were almost similar at low dye concentration (25 mg/L) which meanes removal efficiencies were similar at low dye concentration (25 mg/L) whereas a great difference obtained when the dye concentration reached to 100 mg/l). These phenomena occur because in fixed-bed containing bentonite two processes happened (adoration and photo-Fenton-like experiments) while only photo-Fenton-like process occur in column packed with glass beads. Figure 13 illustrate the interaction effect of flow rate and DB15 concentration fixed-bed glass beads-E@B-Fe/Cu-NPs. Figure 14 and figure 15 illustrate the breakthrough carves for fixed-bed containing glass beads-E@B-Fe/Cu-NPs
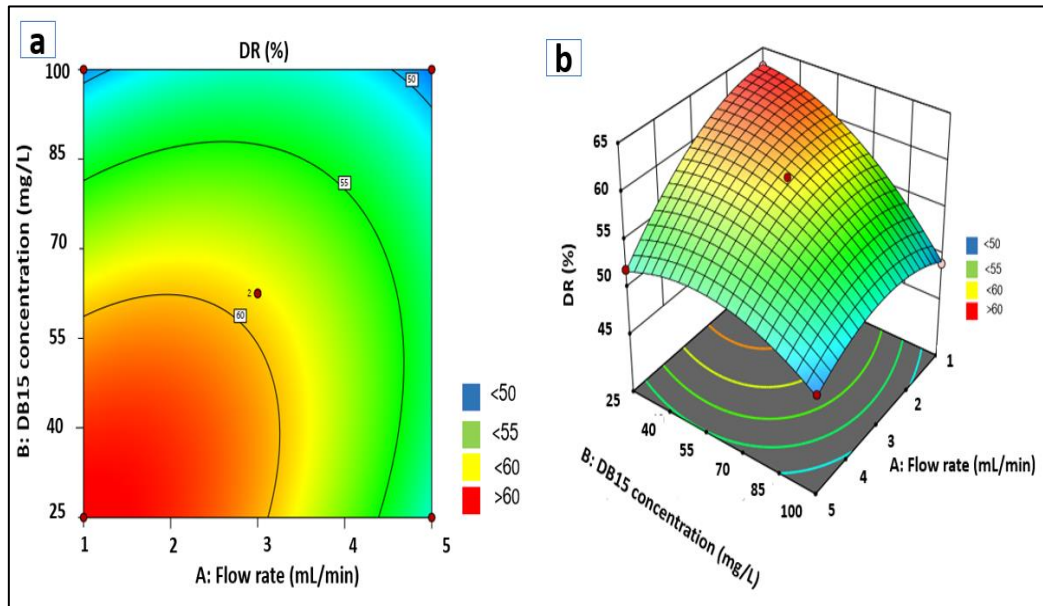
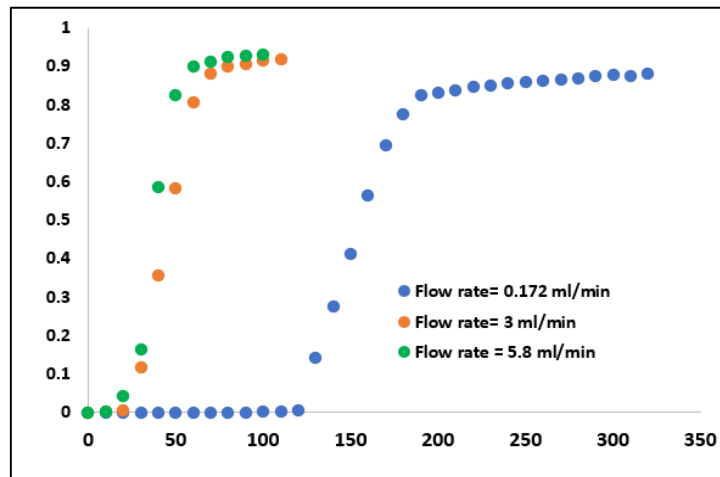**Fig. 13. (a) Contour plot (b) 3D surface of fixed-bed glass beads-E@B-Fe/Cu-NPs.**

Fig. 14. The breakthrough carves at constants DB15 concentration of 626.5 mg/L for fixed-bed column containing glass beads-E@B-Fe/Cu-NPs.
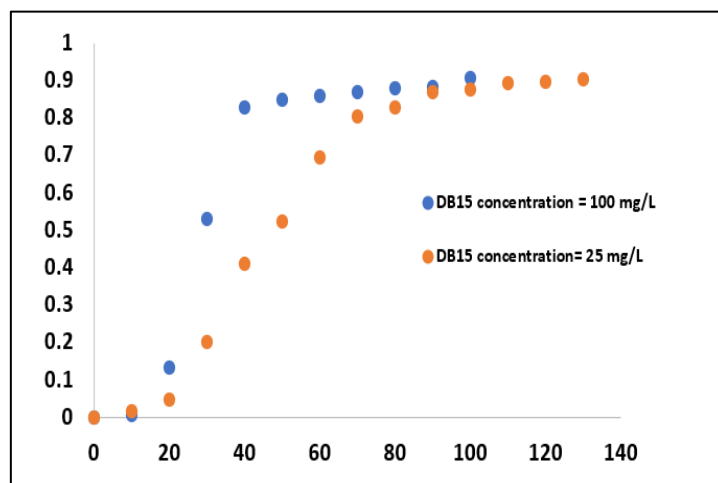

Fig. 15. The breakthrough carves at constants flow rate of 5 ml/min for fixed-bed column containing glass beads-E@B-Fe/Cu-NPs.

Table 8,
Breakthrough results obtaining from fixed-bed glass beads-E@B-Fe/Cu-NPs

EXP. No.	A: Flow rate mL/min	B:DB15 concentration mg/L	DR %	mtotal mg	qtotal mg	tb min	ts min	te min
1	5	100	49	33.56	16.427	12	46.5	95
2	3	62.5	60	14.464	8.668	23.6	64	106.8
3	3	62.5	58.4	14.519	8.37	22.4	61.8	107.2
4	1	25	63	6.832	4.324	98.7	181.6	286.3
5	3	115.533	47	22.795	10.825	14.2	41.2	87.6
6	5.82843	62.5	49	27.941	13.734	14.5	52.3	106.2
7	5	25	52	11.028	5.789	21	66.3	126.2
8	0.171573	62.5	58	2.871	1.789	95.8	166.2	287.1
9	3	9.46699	59	3.579	2.122	42.1	98.6	166.3
10	1	100	49	8.338	4.109	37.1	75.2	152.6

3.5. Optimization of Fixed-bed experiments

Following CCD analysis of the experimental data, the parameters that give the maximum DB15 removal were found, and they are listed in Table 9.

Table 9,
Optimum condition obtained from CCD for fixed-bed containing GB-E@B-Fe/Cu-NPs glass beads-E@B-Fe/Cu-NPs experiments.

Parameters	Flow rate (mL/min)	DB15 concentration (mg/L)	Removal efficiency (%)
	Fixed bed packed with bentonite and E@B-Fe/Cu-NPs		
Optimum condition	1.587	94.213	81.024
	Fixed bed packed with glass beads and E@B-Fe/Cu-NPs		
Optimum condition	1.064	38.37	62.562

4. Conclusion

The characterization results of prepared nanoparticles (E@B-Fe/Cu-NPs) showed that E@B-Fe/Cu-NPs had a spherical shape and porous surface. A zeta potential of -73.25 mV. The E@B-Fe/Cu-NPs surfaces exhibited high roughness. The resultant NPs were used in DB15 degradation through continuous photo-Fenton-like process experiments using a fixed-bed column. Two sets of experiments were designed through central composite design CCD to examine the DB15 degradation through the continuous photo-Fenton-like process using a fixed-bed column. One set involved packing the column with granular bentonite and E@B-Fe/Cu-NPs (GB-Fe/Cu@B-NPs), and the other involved mixing the same catalysts with glass beads (glass beads-Fe/Cu@B-NPs). For GB-Fe/Cu@B-NPs experiments, 94.213 mg/L of DB15 was degraded by 81 % at a flow rate of 1.587 ml/min. The quadratic model describes the effect of parameters on DB15 degradation is given in the equation below.

$$\%DR = 69.5 - 9.6A + 1.88B - 6.5AB - 2.81A^2 + 0.9375B^2$$

On the other hand, the fixed-bed containing glass beads-Fe/Cu@B-NPs exhibited lower DB15 removal efficiency (62.6 % at a flow rate of 1.064 ml/min and DB15 38.37 mg/L) with the quadratic model given in the following equation.

$$\%DR = 59.2 - 2.97A - 4.25B + 2.75AB - 2.85A^2 - 3.1B^2$$

Acknowledgements

5. References

[1] Q. Zhao, J. F. Kennedy, X. Wang, X. Yuan, and B. Zhao, "Optimization of ultrasonic circulating extraction of polysaccharides from Asparagus officinalis using response surface methodology," *Int. J. Biol. Macromol.*, vol. 49, no. 2, pp. 181–187, 2011, doi: 10.1016/j.ijbiomac.2011.04.012.

[2] H. Xiang *et al.*, "Fe3 o4 @c nanoparticles synthesized by in situ solid-phase method for removal of methylene blue," *Nanomaterials*, vol. 11, no. 2, pp. 1–20, 2021, doi: 10.3390/nano11020330.

[3] A. Sengupta and A. Sarkar, Chapter 15 - Green synthesis of nanoparticles: prospect for sustainable efficient photocatalytic dye degradation, First Edit. Elsevier Ltd., 2021.

[4] A. M. Tayeb, M. A. Tony, and S. A. Mansour, "Application of Box–Behnken factorial design for parameters optimization of basic dye removal using nano-hematite photo-Fenton tool," Appl. Water Sci., vol. 8, no. 5, pp. 1–9, 2018, doi: 10.1007/s13201-018-0783-x.

[5] S. Hu, H. Yao, K. Wang, C. Lu, and Y. Wu, "Intensify removal of nitrobenzene from aqueous solution using nano-zero valent iron/granular activated carbon composite as fenton-like catalyst," Water. Air. Soil Pollut., vol. 226, no. 5, 2015, doi: 10.1007/s11270-015-2421-7.

[6] F. Torrades, J. A. García-Hortal, and L. Núñez, "Fenton and photo-Fenton oxidation of a model mixture of dyes - Overall kinetic analysis," Color. Technol., vol. 124, no. 6, pp. 370–374, 2008, doi: 10.1111/j.1478-4408.2008.00165.x.

[7] Y. Gou et al., "Degradation of fluoroquinolones in homogeneous and heterogeneous photo-Fenton processes: A review," Chemosphere, vol. 270, p. 129481, 2021, doi: 10.1016/j.chemosphere.2020.129481.

[8] R. Yamaguchi, S. Kurosu, and M. Suzuki, "Hydroxyl radical generation by zero-valent iron/Cu (ZVI/Cu) bimetallic catalyst in wastewater treatment: Heterogeneous Fenton/Fenton-like reactions by Fenton reagents formed in-situ under oxic conditions," Chem. Eng. J., vol. 334, pp. 1537–1549, 2018, doi: 10.1016/j.cej.2017.10.154.

[9] K. M. Reza, A. Kurny, and F. Gulshan, "Photocatalytic Degradation of Methylene Blue by Magnetite+H2O2+UV Process," Int. J. Environ. Sci. Dev., vol. 7, no. 5, pp. 325–329, 2016, doi: 10.7763/ijesd.2016.v7.793.

[10] C. H. Weng, Y. T. Lin, C. K. Chang, and N. Liu, "Decolourization of direct blue 15 by Fenton/ultrasonic process using a zero-valent iron aggregate catalyst," Ultrason. Sonochem., vol. 20, no. 3, pp. 970–977, 2013, doi: 10.1016/j.ultsonch.2012.09.014.

[11] M. A. Atiya, A. K. Hassan, and F. Q. Kadhim, "Green synthesis of iron nanoparticle using tea leave extract for removal ciprofloxacin (CIP) from aqueous medium," J. Eng. Sci. Technol., vol. 16, no. 4, pp. 3199–3221, 2021.

[12] I. M. Luaibi, M. A. Atiya, A. K. Hassan, and Z. A. Mahmoud, "Heterogeneous catalytic degradation of dye by Fenton-like oxidation over a continuous system based on Box–Behnken design and traditional batch experiments," Karbala Int. J. Mod. Sci., vol. 8, no. 2, pp. 9–28, 2022, doi: 10.33640/2405-609x.3217.

[13] T. Bao et al., "Bentonite-supported nano zero-valent iron composite as a green catalyst for bisphenol A degradation: Preparation, performance, and mechanism of action," *J. Environ. Manage.*, vol. 260, no. January, 2020, doi: 10.1016/j.jenvman.2020.110105.

[14] G. Gopal, H. Sankar, C. Natarajan, and A. Mukherjee, "Tetracycline removal using green synthesized bimetallic nZVI-Cu and bentonite supported green nZVI-Cu nanocomposite: A comparative study," *J. Environ. Manage.*, vol. 254, no. June 2019, p. 109812, 2020, doi: 10.1016/j.jenvman.2019.109812.

[15] X. Weng, Z. Chen, Z. Chen, M. Megharaj, and R. Naidu, "Clay supported bimetallic Fe/Ni nanoparticles used for reductive degradation of amoxicillin in aqueous solution: Characterization and kinetics," *Colloids Surfaces A Physicochem. Eng. Asp.*, vol. 443, pp. 404–409, 2014, doi: 10.1016/j.colsurfa.2013.11.047.

[16] E. S. Önal, T. Yatkin, M. Ergüt, and A. Özer, "Green Synthesis of Iron Nanoparticles by Aqueous Extract of Eriobotrya japonica Leaves as a Heterogeneous Fenton-like Catalyst: Degradation of Basic Red 46," Int. J. Chem. Eng. Appl., vol. 8, no. 5, pp. 327–333, 2017, doi: 10.18178/ijcea.2017.8.5.678.

[17] Z. Wang, C. Fang, and M. Megharaj, "Characterization of iron-polyphenol nanoparticles synthesized by three plant extracts and their fenton oxidation of azo dye," ACS Sustain. Chem. Eng., vol. 2, no. 4,

pp. 1022–1025, 2014, doi:10.1021/sc500021n.

[18] H. M. Abdel-Aziz, R. S. Farag, and S. A. Abdel-Gawad, "Removal of caffeine from aqueous solution by green approach using Ficus Benjamina zero-valent iron/copper nanoparticles," Adsorpt. Sci. Technol., vol. 38, no. 9–10, pp. 325–343, 2020, doi:10.1177/0263617420947495.

[19] G. Ren et al., "Recent advances of photocatalytic application in water treatment: A review," Nanomaterials, vol. 11, no. 7, 2021, doi: 10.3390/nano11071804.

[20] T. Mohapatra, V. Kumar, M. Sharma, and P. Ghosh, "Hybrid Fenton Oxidation Processes with Packed Bed or Fluidized Bed Reactor for the Treatment of Organic Pollutants in Wastewater: A Review," Environ. Eng. Sci., vol. 38, no. 6, pp. 443–457, 2021, doi: 10.1089/ees.2020.0070.

[21] R. Antonelli, G. R. P. Malpass, M. G. C. da Silva, and M. G. A. Vieira, "Fixed-bed adsorption of ciprofloxacin onto bentonite clay: Characterization, mathematical modeling, and DFT-based calculations," Ind. Eng. Chem. Res., vol. 60, no. 10, pp. 4030–4040, 2021, doi: 10.1021/acs.iecr.0c05700.

[22] M. A. Atiya, A. K. Hassan, and I. M. Luaibi, "Green Synthesis Of Bimetallic Iron / Copper Nanoparticles Using Ficus Leaves Extract For Removing Orange G (OG) Dye From Aqueous Medium," Nat. Environ. Pollut. Technol., 2022.

[23] Y. Süzen and C. Ozmetin, "Removal of reactive black 5 dye using fenton oxidation from aqueous solutions and optimization of response surface methodology," Desalin. Water Treat., vol. 172, no. October 2018, pp. 106–114, 2019, doi:10.5004/dwt.2019.24943.

[24] M. R. Sabouri, M. R. Sohrabi, and A. Z. Moghaddam, "A Novel and Efficient Dyes Degradation Using Bentonite Supported Zero-Valent Iron-Based Nanocomposites," ChemistrySelect, vol. 5, no. 1, pp. 369–378, 2020, doi: 10.1002/slct.201904174.

[25] S. C. Azimi, F. Shirini, and A. Pendashteh, "Treatment of wood industry wastewater by combined coagulation–flocculation–decantation and fenton process," Water Environ. Res., vol. 93, no. 3, pp. 433–444, 2021, doi: 10.1002/wer.1441.

[26] D. Solomon, Z. Kiflie, and S. Van Hulle, "Using Box–Behnken experimental design to optimize the degradation of Basic Blue 41 dye by Fenton reaction," Int. J. Ind. Chem., vol. 11, no. 1, pp. 43–53, 2020,

doi:10.1007/s40090-020-00201-5.

[27] D. Charumathi and N. Das, "Packed bed column studies for the removal of synthetic dyes from textile wastewater using immobilised dead C. tropicalis," Desalination, vol. 285, pp. 22–30, 2012, doi: 10.1016/j.desal.2011.09.023.

[28] S. S. Madan, B. S. De, and K. L. Wasewar, "Adsorption performance of packed bed column for benzylformic acid removal using CaO2 nanoparticles," Chem. Data Collect., vol. 23, p. 100267, 2019, doi:10.1016/j.cdc.2019.100267.

[29] V. Parimelazhagan, G. Jeppu, and N. Rampal, "Continuous fixed-bed column studies on congo red dye adsorption-desorption using free and immobilized nelumbo nucifera leaf adsorbent," Polymers (Basel)., vol. 14, no. 1, 2022, doi: 10.3390/polym14010054.

[30] M. Tamez Uddin, M. Rukanuzzaman, M. Maksudur Rahman Khan, and M. Akhtarul Islam, "Adsorption of methylene blue from aqueous solution by jackfruit (Artocarpus heteropyllus) leaf powder: A fixed-bed column study," J. Environ. Manage., vol. 90, no. 11, pp. 3443–3450, 2009, doi: 10.1016/j.jenvman.2009.05.030.

[31] K. Sravanthi, D. Ayodhya, and P. Y. Swamy, "Green synthesis, characterization and catalytic activity of 4-nitrophenol reduction and formation of benzimidazoles using bentonite supported zero valent iron nanoparticles," Mater. Sci. Energy Technol., vol. 2, no. 2, pp. 298–307, 2019, doi: 10.1016/j.mset.2019.02.003.

[32] X. Weng, M. Guo, F. Luo, and Z. Chen, "One-step green synthesis of bimetallic Fe/Ni nanoparticles by eucalyptus leaf extract: Biomolecules identification, characterization and catalytic activity," Chem. Eng. J., vol. 308, pp. 904–911, 2017, doi: 10.1016/j.cej.2016.09.134.

[33] M. J. Khan, K. Shameli, A. Q. Sazili, J. Selamat, and S. Kumari, "Rapid green synthesis and characterization of silver nanoparticles arbitrated by curcumin in an alkaline medium," Molecules, vol. 24, no. 4, 2019, doi: 10.3390/molecules24040719.

[34] S. Raja, V. Ramesh, and V. Thivaharan, "Green biosynthesis of silver nanoparticles using Calliandra haematocephala leaf extract, their antibacterial activity and hydrogen peroxide sensing capability," Arab. J. Chem., vol. 10, no. 2, pp. 253–261, 2017, doi: 10.1016/j.arabjc.2015.06.023.

[35] M. Solís-López, A. Durán-Moreno, F. Rigas,

A. A. Morales, M. Navarrete, and R. M. Ramírez-Zamora, "Assessment of Copper Slag as a Sustainable Fenton-Type Photocatalyst for Water Disinfection," *Water Reclam. Sustain.*, pp. 199–227, 2014, doi:10.1016/B978-0-12-411645-0.00009-2.

[36] M. H. Marzbali and M. Esmaieli, "Fixed bed adsorption of tetracycline on a mesoporous activated carbon: Experimental study and neuro-fuzzy modeling," *J. Appl. Res. Technol.*, vol. 15, no. 5, pp. 454–463, 2017, doi: 10.1016/j.jart.2017.05.003.

[37] F. Farzaneh Kondori, K. Badii, M. E. Masoumi, and G. Golkarnarenji, "A novel continuous magnetic nano-Fe3O4/perlite fixed bed reactor for catalytic wet peroxide oxidation of dyes: reactor structure," *Int. J. Environ. Sci. Technol.*, vol. 15, no. 3, pp. 543–550, 2018, doi: 10.1007/s13762-017-1420-1.

تأثير المادة الداعمة على تحطيم صبغة الازو بواسطة عملية (photo-Fenton-like) وباستخدام العمود المتسمر ذو الحشوة الثابتة

زينب عادل محمود *   محمد عبد عطية السراج**   احمد خضير حسان***

*،*** قسم الهندسة الكيميائية الاحيائية/ كلية الهندسة الخوارزمي/ جامعة بغداد/ العراق

** دائرة بحوث البيئة والمياه/ وزارة العلوم والتكنولوجيا / العراق

الخلاصة

في هذا الدراسة تم استخدام نظام الدفعات المستمرة وعملية (Photo-Fenton-like) لمعالجة مياه الصرف الصحي الملوثة بصبغة زرقاء المعروفة باسم (Direct blue 15). تم استخدام مستخلص أوراق الأوكالبتوس لإنشاء جسيمات نانوية ثنائية المعدن من الحديد / النحاس وتم تحميلها على طين البنتونايت لاستخدامها كمحفزات غير متجانسة. تمت دراسة ومقارنة تكوينين من العمود ذو الحشوة الثابتة. الأول يتضمن خلط البنتونايت الحبيبي مع المحفز واستخدامه كحشوة للعمود، والآخر تضمن خلط المحفز مع الخرز الزجاجية. تم تطبيق طرق التوصيف على الجسيمات النانوية الناتجة، بما في ذلك المسح المجهري الإلكتروني SEM، وإمكانات زيتا ((Zeta potential، وتقنيات التحليل الطيفي للقوى الذرية (AFM). تم دراسة تأثير العوامل الرئيسية على التحلل الصبغة اهمها معدل التدفق، وتركيز الصبغة. تم استخدام منهجية سطح الاستجابة القائمة على التصميم المركب المركزي (CCD) لمعرفة الظروف المثلى لكلا النظامين المدروسين. أظهرت النتائج أن كفاءة الإزالة كانت 81٪ في العمود الذي يحتوي على حبيبات البنتونايت مع المحفز و62.6٪ في العمود الذي يحتوي على الخرز الزجاجية مع المحفز.